Impact of Mobility in Spectrum Sensing Capacity

Luis Irio[1,2(✉)] and Rodolfo Oliveira[1,2]

[1] IT, Instituto de Telecomunicações, Lisbon, Portugal
[2] Departamento de Engenharia Electrotécnica,
Faculdade de Ciências Tecnologia, FCT,
Universidade Nova de Lisboa, 2829-516 Caparica, Portugal
l.irio@campus.fct.unl.pt

Abstract. This work evaluates the secondary users' (SUs) transmission capability considering that the primary users (PUs) can move to different positions. The transmission capability identifies the available opportunities for SU's transmission. No opportunities are available when mobile PUs are active within the SU's sensing region. We also consider the scenario when the PUs are undesirable detected active when they are not located within the SUs' sensing region. Our analysis indicate that the transmission capability increases as the average mobility of the PUs decreases, which is confirmed by simulation.

Keywords: Cognitive Radio Networks · Spectrum Sensing · Mobility

1 Introduction

In Cognitive Radio Networks (CRNs), the non-licensed users usually denominated Secondary Users (SUs) must detect the activity of the licensed users, denominated Primary Users (PUs), in order to utilize the unused spectrum bands without causing them harmful interference. Spectrum Sensing (SS) plays a central role in CRNs, since it allows to detect portions of spectrum available for transmission in the spatial sensing area of a SU. Several SS techniques were already studied and reported in the literature [1], including Waveform-based sensing [3], Energy-based sensing (EBS) [2], Cyclostationarity-based sensing (CBS) [5], and Matched Filter-based sensing (MFBS) [4]. Different surveys focused on spectrum sensing techniques are already available (e.g. [6, 7]).

Due to the path loss effect it is more difficult to detect the activity of the PUs when they move across a given region. Consequently, is more difficult to characterize the transmission capability of the SUs, denoted as Sensing Capacity (SC), when mobile PUs are considered. For static CRNs, where the nodes stay at the same position, the SC metric was defined in [8] as

$$C^{static} = \eta \cdot \zeta \cdot W \cdot P_{off}, \tag{1}$$

where η denotes the sensing efficiency, W represents the bandwidth, ζ represents the spectral efficiency of the band (bit/sec/Hz), and P_{off} is the probability of the band being

P. Marques et al. (Eds.): CROWNCOM 2017, LNICST 228, pp. 162–172, 2018.
https://doi.org/10.1007/978-3-319-76207-4_14

accessible to SUs due to the inactivity of PUs. More recently, the SC was defined considering that several PUs act as mobile nodes [9, 10],

$$C^{mob} = \eta \cdot \zeta \cdot W \cdot P_{\mathcal{I}_{off}}, \tag{2}$$

where $P_{\mathcal{I}_{off}}$ is the probability of inactivity (i.e. not transmitting) of the PUs positioned over the SU's sensing region. While admitting multiple PUs and mobile scenarios, the SC defined in [9, 10] is not including the case when the PUs are located outside the SU's sensing region and may be anomaly detected. This effect, denominated Spatial False Alarm (SFA) effect [11], is related with the behavior of a SU misunderstanding a non-interfering PU, and was recently studied in [12] considering multiple static PUs. The SC expressed in (2) is an upper bound, because no SFA is considered. Differently from [9, 10], this work considers that the SFA effect may occur in a CRN with multiple mobile PUs, being the SC now defined as

$$C_{SFA}^{mob} = \eta \cdot \zeta \cdot W \cdot \left(P_{\mathcal{O}_{SFA}} \cdot P_{\mathcal{I}_{off}}\right), \tag{3}$$

where $P_{\mathcal{O}_{SFA}}$ is the probability of not occurring the SFA effect due to the activity of the nodes located outside the SU's sensing region.

The characterization of the sensing capacity when both mobility [9, 10] and SFA effects [11, 12] are considered has not been addressed before. The contributions of this work are summarized as follows:

- The spatial false alarm probability is derived by characterizing the aggregate interference originated by the mobile PUs not located within the SU's sensing region (i.e. when the PUs are located outside);
- The SC of CRNs, defined in [9, 10], is extended to consider the SFA effect. Both simulation and theoretical results show that SFA should not be neglected.
- We confirm that the SFA effect decreases the SC, and the results in [8–10] represent a SC's upper bound;
- Regarding the mobility of the nodes, it is shown that the SC varies inversely with the average speed of the PUs.

The paper is organized as follows. Section 2 characterizes the PUs' mobility model. The interference caused by the PUs to a SU is tackled in Sect. 3. The sensing capacity is analyzed in Sect. 4. Finally, conclusions are presented in Sect. 5.

2 System Model

2.1 System Description

This work considers that PUs are mobile nodes that move according to the Random WayPoint (RWP) mobility model [13]. By considering the RWP mobility model, we assume that n PUs move in a rectangular region with area $X_{max} \times Y_{max}$. The mobility is treated individually, and each PU is placed in a random location (x, y) in the beginning of simulation. The location of PUs is sampled from the uniform distribution characterized by $x \in [0, X_{max}]$ and $y \in [0, Y_{max}]$. (x, y) denotes the departing point.

The destination point (x', y') is also uniformly chosen as the departing point (*i.e.* $x' \in [0, X_{max}]$ and $y' \in [0, Y_{max}]$). After defining the departure and destination points a PU uniformly chooses the velocity $v \in [V_{min}, V_{max}]$ to move to the ending point. After reaching the ending point (x', y'), a PU randomly chooses a pause duration $\left(T_p \in [0, T_{P_{max}}]\right)$, and during this period of time it stays at the ending point. After elapsing T_p, a PU uniformly chooses a new velocity value to move to another ending point uniformly chosen. After reaching the ending point a PU repeats the same cycle as many times as required. Nodes move with expected velocity E[V].

Figure 1 represents the system considered in this work. The static SU N_c is placed in the center of the considered scenario (in the position $(X_{max}/2, Y_{max}/2)$), and N_c senses the activity of the mobile PUs located in the circular sensing region with radius R_i^1 (characterized by the dark disk involving N_c). This work considers the SU's sensing region concept instead of the PU's protection region. However, both concepts are equivalent if the PU's protection range is equal or smaller than the SU's sensing range.

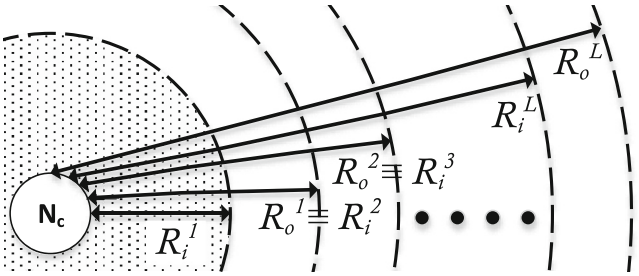

Fig. 1. Spatial scenario considered. The sensing region of the SU (node N_c) is represented by the area $A_{SR} = \pi(R_i^1)^2$.The PUs located outside the sensing region are found in the area given by $A = \pi\left((R_o^L)^2 - (R_i^1)^2\right)$.

2.2 Distribution of the PUs Over the Simulated Region

The annulus area $A = \pi\left((R_o^L)^2 - (R_i^1)^2\right)$ in Fig. 1 can be obtained via calculus by dividing the annulus up into an infinite number of annuli of infinitesimal width $d\chi$ and area $2\pi\chi d\chi$ and then integrating from $\chi = R_i^1$ to $\chi = R_o^L$, i.e. $A = \int_{R_i^1}^{R_o^L} 2\pi\chi\, d\chi$. Using the Riemann sum, A can be approximated by the sum of the area of a finite number (L) of annuli of width ρ,

$$A \approx \sum_{l=1}^{L} A_l, \tag{4}$$

where $A_l = \pi\left((R_o^l)^2 - (R_i^1)^2\right)$ represents the area of the annulus l, $l \in \{1, ..., L\}$. $R_o^l = \left(R_i^1 + l\rho\right)$ and $R_i^l = \left(R_i^1 + (l-1)\rho\right)$ denotes the radius of the larger circle and smaller circle of the annulus l, respectively.

In a specific annulus l, the number of PUs is represented by the random variable (RV) X_l and is approximately described by a Poisson distribution with Probability Mass Function (PMF)

$$P(X_l = k) \approx \frac{(\beta_l A_l \tau)^k}{k!} e^{-\beta_l A_l \tau}, k = 0, 1, \ldots, n, \tag{5}$$

where β_l represents the spatial density of the PUs located in the annulus l, the number of PUs is represented by n and the probability of the PUs being active is denoted by τ. By dividing the area A in the multiple areas A_l, a different β_l is considered for each annulus A_l, which better approximates the spatial distribution of PUs in the area A.

The spatial distribution of the PUs in two dimensions (x and y) follows the result in [14, Theorem 3, $\alpha = 2$] and is given by

$$f_{XY}(x, y) = \frac{p_p}{a^2} + (1 - p_p)\frac{36}{a^4}\left(\frac{x^2}{a} - \frac{a}{4}\right)\left(\frac{y^2}{a} - \frac{a}{4}\right),$$

for $-a/2 \leq x \leq a/2, -a/2 \leq y \leq a/2, a = X_{\max} = Y_{\max}$ and where

$$p_p = \frac{(V_{max} - V_{min})E[T_p]}{0.521405 \times a \times \ln\left(\frac{V_{max}}{V_{min}}\right) + (V_{max} - V_{min})E[T_p]}.$$

The location of a PU within the annulus l is represented by the Bernoulli RV X_b^l and the probability of a PU being positioned within the l–th annulus is given by

$$P(X_b^l = 1) = \int_{-R_o^l}^{R_o^l} \int_{-\sqrt{(R_o^l)^2 - x^2}}^{\sqrt{(R_o^l)^2 - x^2}} v - \int_{-R_o^l}^{R_i^l} \int_{-\sqrt{(R_i^l)^2 - x^2}}^{\sqrt{(R_i^l)^2 - x^2}} v, \tag{6}$$

with $v = f_{XY}(x, y)\, dy\, dx$. The PU's spatial density of the annulus l, defined as β_l in (5), is given by $\beta_l \approx nP(X_b^l = 1)/A_l$, where $nP(X_b^l = 1)$ represents the average number of nodes located in the area A_l. In what follows (5) is adopted to characterize the number of PUs placed over the multiple annuli (L).

3 Aggregate Interference

3.1 Interference Caused by the PUs Located Within the l–th Annulus

The aggregate interference power received by the secondary user N_c placed in the center of the l–th annulus is given by

$$I = \sum_{i=1}^{n_l} I_i, \tag{7}$$

where n_l is the total number of PUs located in the annulus and I_i is the interference caused by the i-th PU. The individual interference power I_i is expressed by

$$I_i = P_{Tx}\psi_i r_l^{-\alpha}, \tag{8}$$

where P_{Tx} is the transmission power of the i-th PU[1], ψ_i is the fading observed in the channel between the PU i and SU, and r_l represents the distance between the i–th interferer and the receiver. The path-loss coefficient is represented by α.

The moment generating function (MGF) of the aggregate interference due to path loss ($\psi_i = 1$) is derived in the next steps. Let $M_I^i(s)$ denote the MGF of the i-th PU ($i = 1, \ldots, n_l$) positioned over the annulus l, given by

$$M_I^i(s) = E_{I_i}\left[e^{sI_i}\right], \tag{9}$$

where E_{I_i} denotes the expectation of I_i. The PDF of r_l can be written as the ratio between the perimeter of the circle with radius r_l and the total area A_l, being represented as follows

$$f_R(r_l) = \begin{cases} \frac{2\pi r_l}{A_l}, & R_i^l < r_l < R_o^l \\ 0, & otherwise \end{cases}. \tag{10}$$

Using (8) and (10) the MGF of the interference power received by the node N_c caused by the i-th PU is represented by

$$M_I^i(s) = \frac{2P_{Tx}^{2/\alpha}\left(\Gamma\left(-2/\alpha, P_{Tx}(R_o^l)^{-\alpha}\right)s\right) - \Gamma\left(-2/\alpha, P_{Tx}(R_i^l)^{-\alpha}s\right)\right)}{\left((R_o^l)^2 - (R_i^1)^2\right)s},$$

where $\Gamma(s,x) = \int_x^\infty t^{s-1}e^{-t}dt$ is the upper incomplete gamma function and $\Gamma(s) = \int_0^\infty t^{s-1}e^{-t}dt$ represents the gamma function.

The PDF of the aggregate interference I due to k active PUs may be defined though the convolution of the PDFs of each I_i, when the individual interference I_i is independent and identically distributed. Consequently, the MGF of I is written as follows

$$M_{I/k}(s) = M_I^1(s) \times \cdots \times M_I^k(s) = \left(M_I^i(s)\right)^k. \tag{11}$$

The PDF of the aggregate interference (I) may be stated through the Law of Total Probability as follows

[1] For every PU we have assumed $P_{Tx} = 10^3$ mW.

$$f_I(j) = \sum_{k=0}^{n_l} f_I(j|X_l = k)P(X_l = k), \tag{12}$$

leading to the MGF of the aggregate interference, I, which can be written as

$$\mathrm{E}\left[e^{sI}\right] = \sum_{k=0}^{n_l} P(X_l = k)M_{I/k}(s). \tag{13}$$

Using (11), the MGF of I is given as follows

$$\mathrm{E}\left[e^{sI}\right] = \sum_{k=0}^{n_l} P(X_l = k)e^{k\,ln\left(M_l^i(s)\right)} = e^{\beta_l A_l \tau\left(M_l^i(s)-1\right)}. \tag{14}$$

The expectation of the aggregate interference, E[I], can be obtained using the Law of Total Expectation, i.e.,

$$\mathrm{E}[I] = \mathrm{E}[\mathrm{E}[I|X_l]] = 2\pi\beta_l\tau P_{Tx}\left(\frac{(R_o^l)^{2-\alpha} - (R_i^l)^{2-\alpha}}{2-\alpha}\right). \tag{15}$$

Similarly, the variance of the aggregate interference can be obtained using the Law of Total Variance as follows

$$\mathrm{Var}[I] = \mathrm{Var}[I_i]\mathrm{E}[X_l] + \mathrm{E}[I_i]^2\mathrm{Var}[X_l]. \tag{15}$$

Since X_l is distributed according to a Poisson distribution (with mean $\beta_l A_l \tau$), the variance of the aggregate interference is expressed by

$$\mathrm{Var}[I] = \pi\beta_l\tau P_{Tx}^2\left(\frac{(R_o^l)^{2-2\alpha} - (R_i^l)^{2-2\alpha}}{1-\alpha}\right)$$

As shown in [15], the aggregate interference due to path loss can be approximated by a Gamma distribution. Consequently the shape and the scale parameters of the Gamma distribution, denoted by k_l and θ_l, are respectively given by $k_l = \mathrm{E}[I]^2/\mathrm{Var}[I]$ and $\theta_l = \mathrm{Var}[I]/\mathrm{E}[I]$.

3.2 Aggregate Interference Due to PUs Located Within L Annuli

As shown in the previous subsection, the interference I caused to the N_c by the PUs located within the l-th annulus is approximated by a gamma distribution, with MGF

$$M_I^l(s) = (1 - \theta_l s)^{-k_l}. \tag{16}$$

The annulus of width $R_o^L - R_i^1$ s can be expressed as a summation of L annuli of width ρ. Consequently, the MGF of the aggregate interference originated by the PUs positioned over the L annuli is represented by

$$M_{I_{agg}}(s) = \prod_{l=1}^{L} (1 - \theta_l s)^{-k_l}. \tag{17}$$

3.3 Distribution of the Aggregate Interference

The interference due to the PUs located outside the SU's sensing region can be seen as the summation of the L individual aggregated interferences caused by the PUs located within L annuli. Therefore, the expressions for the cumulative distribution function (CDF) and the PDF of the summation of L independent gamma random variables are given in [16].

Defining $\{X_l\}_{l=1}^{L}$ as independent gamma variables, but not necessarily identically distributed with parameters θ_l (scale) and k_l (shape), then the PDF of $I_{agg} = \sum_{l=1}^{L} X_l$ can be expressed as [16]

$$f_{I_{agg}}(s) = \prod_{l=1}^{L} \left(\frac{\theta_1}{\theta_l}\right)^{k_l} \sum_{w=0}^{\infty} \frac{\delta_w s^{\left(\sum_{l=1}^{L} k_l + w - 1\right)} \exp\left(-\frac{s}{\theta_1}\right)}{\theta_1^{\left(\sum_{l=1}^{L} k_l + w\right)} \Gamma\left(\sum_{l=1}^{L} k_l + w\right)}, \tag{18}$$

where $\theta_1 = \min_l\{\theta_l\}$, and the coefficients δ_w are obtained recursively,

$$\delta_{w+1} = \frac{1}{w+1} \sum_{i=1}^{w+1} \left[\sum_{l=1}^{L} k_l \left(1 - \frac{\theta_1}{\theta_l}\right)^i\right] \delta_{w+1-i},$$

and $\delta_0 = 1$. Γ (.) represents the gamma function.

4 Sensing Capacity

4.1 Formal Definition

The band licensed of the PUs is sensed by a SU to evaluate if the spectrum is vacant or occupied. The sensing decision considered in this work is computed periodically (a period of 1 s was adopted) having the amount of aggregate interference sensed outside the sensing region into account.

Departing from the definition of SC in (3), we first define $P_{\mathcal{I}_{off}}$, the probability of not occurring any activity caused by the PUs that may be located within the SU's sensing region. A PU is located within the SU's sensing region with probability $P_{\mathcal{I}}$ given by

$$P_{\mathcal{I}} = \int_{-R_i^1}^{R_i^1} \int_{-\sqrt{\left(R_i^1\right)^2 - x^2}}^{\sqrt{\left(R_i^1\right)^2 - x^2}} f_{XY}(x, y) dy dx. \tag{19}$$

Because all PUs move independently, the probability of $k \leq n$ PUs being positioned over the sensing region of the SU is expressed by the probability mass function

$$B(n, k, P_{\mathcal{I}}) = \binom{n}{k} (P_{\mathcal{I}})^k (1 - P_{\mathcal{I}})^{(n-k)}. \tag{20}$$

Finally, $P_{\mathcal{I}_{off}}$ is defined as

$$P_{\mathcal{I}_{off}} = \sum_{k=0}^{n} B(n, k, P_{\mathcal{I}}) \cdot (1 - \tau)^k, \tag{21}$$

since the k PUs within the sensing region of the SU are inactive with probability $(1 - \tau)^k$.

Regarding $P_{\mathcal{O}_{SFA}}$ in (3), which denotes the probability of not occurring SFA due to the PUs located outside the SU's sensing region, and following the notation in (21) we start to consider that $n - k$ PUs are located outside the sensing region. A spatial false alarm does not occur if the aggregate interference power caused by the PUs located outside the sensing region is lower than a given threshold (γ). Its probability is represented by $P\ (I_{agg}\ \{n_l = n - k\} \leq \gamma)$, where $\{n_l = n - k\}$ indicates that the parameters k_l and θ_l must be computed assuming n_l defined in Sect. 3.1 equal to $n - k$. After computing the parameters k_l and θ_l, $f_{Iagg}\ (s)$ may be also computed through (18) and

$$P\left(I_{agg}\{n_l = n - k\} \leq \gamma\right) = \int_0^{\gamma} f_{I_{agg}}(s) ds. \tag{22}$$

By considering the different number of $n - k$ PUs that may be localized outside the session region, $P_{\mathcal{O}_{SFA}}$ is given by

$$P_{\mathcal{O}_{SFA}} = \sum_{k=0}^{n} \left(I_{agg}\{n_l = n - k\} \leq \gamma\right), \tag{23}$$

and finally using (3), (21) and (23), the sensing capacity is written as follows

$$C_{SFA}^{mob} = \eta \cdot \zeta \cdot W \sum_{k=0}^{n} B(n, k, P_{\mathcal{I}}) \cdot (1 - \tau)^k \cdot P\left(I_{agg}\{n_l = n - k\} \leq \gamma\right). \tag{24}$$

Table 1. Parameters used to compute the different results.

^{X}max	1000 m	R_i^1	100 m	α	2
^{Y}max	1000 m	$T_{P_{max}}$	0 s, E[V] = 10.82 m/s	ρ	10 m
^{V}min	5 m/s	$T_{P_{max}}$	300 s, E[V] = 1.50 m/s	L	61
^{V}max	20 m/s	$\eta \cdot \zeta \cdot W$	1	γ	0.1 mW

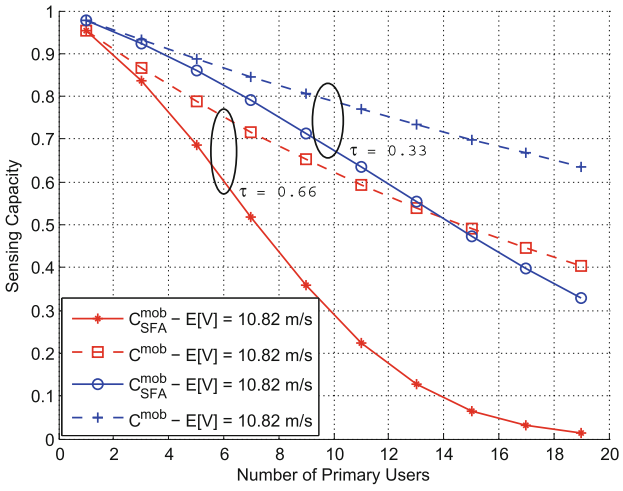

(a)

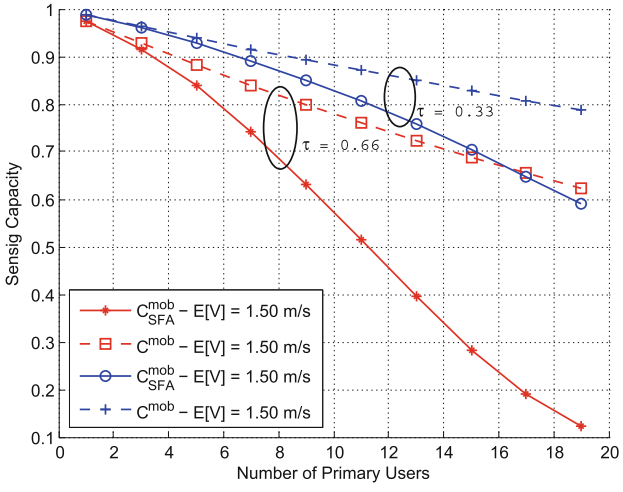

(b)

Fig. 2. Sensing capacity for different levels of PU's activity (τ): (a) high mobility scenario (E[V] = 10.82 m/s); (b) low mobility scenario (E[V] = 1.50 m/s).

4.2 Comparison Results

This subsection compares the impact of the SFA in the SU's SC. The SC is computed with (24) and compared with the results obtained with (27) in [9] (similar to (2)), which neglects the SFA effect. Different network scenarios were considered, where the number of mobile PUs were varied from a single PU to 19. The PUs moving according to the RWP mobility model achieve different average velocities, E[V] = {1.50, 10.82} m/s, by adopting $T_{P_{max}} = \{0, 300\}$ s, respectively. Two different probabilities of PU's activity were also considered, i.e. $\tau = \{0.33, 0.66\}$. The simulations were run for each number of PUs and adopting constant $T_{P_{max}}$ and τ values. The missing parameters related with the propagation model and the computation of theoretical model are described in Table 1.

The sensing capacity results (computed with (24) and (27) in [9]) are illustrated in Fig. 2. Figure 2(a) plots the results for E[V] = 10.82 m/s, while 2(b) plots the result for E[V] = 1.50 m/s. Regarding the impact of the PUs' mobility on the SC, it is well known that the spatial density of the nodes moving according the RWP model increases within the sensing region of the node N_C as the average velocity of the nodes increase [14]. Consequently, more PUs are likely to be located within the sensing region as the average velocity of the PUs increases. In this case, the node N_c detects higher PUs' activity within its sensing region, leading to a lower SC (Fig. 2(a)), when compared to a scenario of lower average velocity (Fig. 2(b)).

Finally, the results presented in Fig. 2 show that for the two assumptions (considering/neglecting the SFA) the SC varies inversely with the number of PUs, the level of PU's activity (τ), and the average velocity of the PUs (E[V]). However, the SC decreases more sharply when the SFA effect is considered, and the deviation from neglecting the SFA increases when the number of PUs and PU's level of activity increase, or when the average velocity of the nodes decrease. Moreover, the deviation observed in the SC confirms that when the SFA effect is neglected the results obtained with [9] represent an upper bound of the SC.

5 Conclusions

This work characterizes the SUs sensing capacity in a CRN when are considered multiple mobile PUs. Contrarily to other works, we consider that PUs may be detected active when they are located outside the sensing region. This effect, known as SFA, degrades the sensing capacity of CRs, as demonstrated in the paper. Moreover, it is shown that the decrease of the sensing capacity due to the SFA effect may be significant, namely when the PU's activity and the number of PUs increase. Finally, due to the mobility model, the results presented in the paper indicate that the sensing capacity increases as the average velocity of the nodes decrease. This result indicates that the capacity of the SUs varies inversely with the velocity of the PUs, which confirms the importance of this work.

Acknowledgments. This work was partially supported by the Portuguese Science and Technology Foundation (FCT/MEC) under the project UID/EEA/50008/2013 and grant SFRH/BD/108525/2015. The work was also supported by the "Faculdade de Cincias e Tecnologia" - Nova University of Lisbon, through the PhD Program in Electrical and Computer Engineering.

References

1. Yucek, T., Arslan, H.: A survey of spectrum sensing algorithms for cognitive radio applications. IEEE Commun. Surv. Tutorials **11**, 116–130 (2009)
2. Urkowitz, H.: Energy detection of unknown deterministic signals. Proc. IEEE **55**, 523–531 (1967)
3. Zahedi-Ghasabeh, A., Tarighat, A., Daneshrad, B.: Spectrum sensing of OFDM waveforms using embedded pilots in the presence of impairments. IEEE Trans. Veh. Technol. **61**, 1208–1221 (2012)
4. Bouzegzi, A., Ciblat, P., Jallon, P.: Matched filter based algorithm for blind recognition of OFDM systems. In: Proceedings of IEEE VTC 2008-Fall, pp. 1–5, September 2008
5. Al-Habashna, A., Dobre, O.A., Venkatesan, R., Popescu, D.C.: Cyclostationarity- based detection of LTE OFDM signals for cognitive radio systems. In: Proceedings of IEEE GLOBECOM 2010, pp. 1–6, December 2010
6. Masonta, M.T., Mzyece, M., Ntlatlapa, N.: Spectrum decision in cognitive radio networks: a survey. IEEE Commun. Surv. Tutorials **15**, 1088–1107 (2013)
7. Sun, H., Nallanathan, A., Wang, C.-X., Chen, Y.: Wideband spectrum sensing for cognitive radio networks: a survey. IEEE Wirel. Commun. **20**, 74–81 (2013)
8. Lee, W.-Y., Akyildiz, I.F.: Optimal spectrum sensing framework for cognitive radio networks. IEEE Trans. Wireless Commun. **7**, 3845–3857 (2008)
9. Cacciapuoti, A.S., Akyildiz, I.F., Paura, L.: Primary-user mobility impact on spectrum sensing in cognitive radio networks. In: 22nd IEEE International Symposium on Personal, Indoor and Mobile Radio Communications, pp. 451–456, Toronto (2011)
10. Cacciapuoti, A.S., Akyildiz, I.F., Paura, L.: Optimal primary-user mobility aware spectrum sensing design for cognitive radio networks. IEEE J. Sel. Areas Commun. **31**, 2161–2172 (2013)
11. Han, W., Li, J., Liu, Q., Zhao, L.: Spatial false alarms in cognitive radio. IEEE Commun. Lett. **15**, 518–520 (2011)
12. Han, W., Li, J., Li, Z., Si, J., Zhang, Y.: Spatial false alarm in cognitive radio network. IEEE Trans. Sig. Process. **61**, 1375–1388 (2013)
13. Johnson, D.B., Maltz, D.A.: Dynamic source routing in ad hoc wireless networks. Mob. Comput. **353**, 153–181 (1996)
14. Bettstetter, C., Resta, G., Santi, P.: The node distribution of the random way- point mobility model for wireless ad hoc networks. IEEE Trans. Mob. Comput. **2**, 257–269 (2003)
15. Haenggi, M., Ganti, R.K.: Interference in large wireless networks. Found. Trends Netw. **3**, 127–248 (2009)
16. Moschopoulos, P.G.: The distribution of the sum of independent gamma random variables. Ann. Inst. Stat. Math. **37**, 541–544 (1985)